ISTITUTO NAZIONALE FISICA NUCLEARE

INFN/TC - 83/1

15 gennaio 1983

L. Bacarini, A. Di Lelio, R. Giacomich and F. Tomasini:

LIGHT PRODUCTION FROM Gd_2O_2S INTENSIFYING SCREENS

SERVIZIO RIPRODUZIONE DELLA

SEZIONE DI TRIESTE DELL'INFN

LIGHT PRODUCTION FROM Gd_2O_2S INTENSIFYING SCREENS

R. Giacomich
Istituto di Fisica, Università di Trieste
Istituto Nazionale Fisica Nucleare - Sezione di Trieste

F. Tomasini
Istituto Nazionale Fisica Nucleare - Sezione di Trieste

L. Bacarini
Servizio di Radiodiagnostica, Ospedali Riuniti di Trieste

A. Di Lelio
Servizio di Radiodiagnostica, Ospedali Riuniti di Trieste

ABSTRACT

All five 3M screens of the TRIMAX series were evaluated.

The physical parameters of absorption and the light conversion efficiency have been measured by means of a NaI spectrometer and the SPC technique. This allowed to calculate the number of light photons emitted per incident X-ray having different energies (from 10 to 120 keV), and therefore the total efficiency curves ("Absolute Speed Curve" ASC). The phenomenon of ionization energy loss due to fluorescent X-rays production for incident X-rays having an energy above the K-edge of the Gd, was evaluated as well as the particular behaviour of the T_{16B} whose high thickness makes the phenomena of internal light and fluorescent X-ray absorption important

INTRODUCTION

The purpose of this paper is to report experimental measures aimed at defining the efficiency of light conversion of Gd_2O_2S intensifying screens (IS) as used by diagnostic radiology ([1]). Commercially available TRIMAX IS by 3M were here tested.

In this paper, efficiency of light conversion means the average number of light photons emitted by each X-ray absorbed.

Conversion efficiency may be obtained starting from the amount of energy taken by the screen from the X-ray absorbed in the bulk of the phosphor. This data may easily be found from total and absorption cross section values, as widely reported in the literature ([2,3,4]).

This theoretical approach to the problem does not supply the effective number of light photons emitted by each absorbed X-ray, but only an overall description of the phenomenon; in addition it does not take into account some peculiar aspects of the phenomenon such as the self-absorption of light by screens and the escape of photoelectrons from the screen itself.

CHAPTER 1

LIGHT EMISSION PROCESSES.

The emission of light from an intensifying screen as consequence of absorption of X-rays is the result of a number of physical processes which have been throughly described by several authors.

The whole process may be described as 4 interconnected stages.

The first stage is the interaction of the X-ray with the material constituting the screen. Our interest is limited to the range of energies 10 to 100 keV which is the range commonly used in diagnostic radiology. The main kind of the above mentioned interactions in this range is the photoelectric effect. Since the photoelectric cross-section is in ratio to Z^4 we can safely consider the effect limited to the atoms of Gd.

The energy of the emitted photoelectrons is $T = h\nu - B_e$ where B_e is the binding energy of the electrons involved, which are usually K or L.

The second stage involves the atom returning to its ground state by a series of processes which have as result the emission of fluorescent X-rays and Auger electrons.

According to (2), we can assume that all X_L and the following X_M are immediately reabsorbed; only $X_{K\alpha}$ and $X_{K\beta}$, in view of their energy, escape from the site of primary interaction and, as a result, energy is lost in the process.

The third stage is the ionization caused by the photo-electrons, the Auger electrons and the fluorescent X-ray reabsorption.

At this point we have a loss of energy due to the high probability that the most energetic electrons, in their motion, escape from the screen; the thinnest screen, in fact, is 21,5 mg/cm^2

thick and this value is comparable to the range of electrons in the material of the screen itself (100 keV electron has a range of about 15 mg/cm^2). This escape is another cause of loss of energy.

The fourth and last stage involves the conversion of ionization energy into light in the luminescence centres of Tb and the following propagation of light from the emitting point out of the screen.

This stage was described by ([5]) who simulated the process on the computer by the Monte Carlo method and related the dependence of the emission of light to the size of the Gd_2O_2S grain.

Based on the above we believe it relevant to show the diagrams describing X-ray interaction with Gd (Fig. 1).

The graph relates cross-section for photoelectric effect to cross-section of photoelectric effect with energy absorption.

We do not feel it relevant to mention the cross-section of Rayleigh since in the Rayleigh scattering we do not have energy transfer but only minor deviation of incident X-rays which therefore do not affect the beam, leaving it practically unchanged.

The absorption cross-section differs only slightly from the total cross-section below the K-edge of Gd (50,2 KeV) but in the hypothesis reported by ([2]) it has practically the same value.

This data are different from that reported by ([2]), due to the different hypothesis used to describe the mechanism of fluorescent X-ray escape ([3]). Fig. 2 shows the relationship between E and σ_A/σ_{tot}; the function $\sigma_A/\sigma_{tot} \times E$ gives the fraction of average energy left in the screen by an X-ray having energy E. Therefore in the hypothesis that the emission of light is proportional to the absorbed energy, the graph also represents the pattern of the curves of light emission from the screens in absence of other losses.

Above the K-edge, data from ([4]) takes into account the escape of fluorescent X-rays from the K-shell showing the great difference between σ_{total} and $\sigma_{absorption}$.

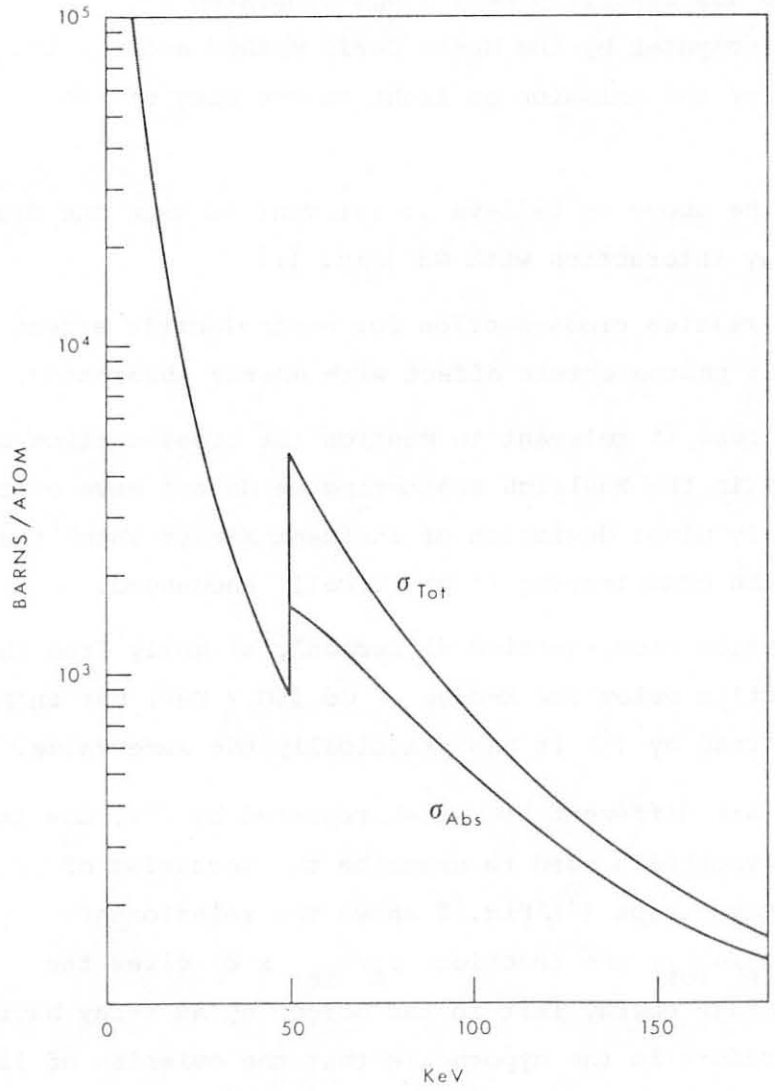

Fig. 1 - Total cross-section (σ_{tot}) and total cross-section with energy absorption (σ_{ABS}) for Gd expressed in barns/atom as a function of energy.

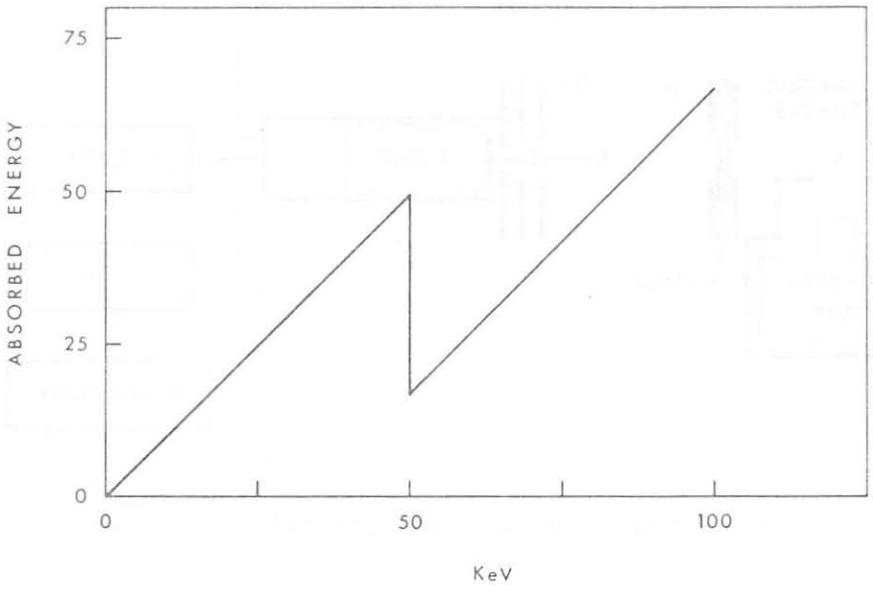

Fig. 2 - Effective energy absorption per interacting X-rays of energy E, as function of X-photon energy.

CHAPTER 2

EXPERIMENTAL PROCEDURE.

The purpose of the measures carried out, was to obtain experimentally the average number of photons emitted by every X-ray absorbed by the screens, as a function of the incident X-ray energy. This is done by measuring the spectrum of light pulse height.

For this purpose the single photon counting technique was used. A specimen of the screen being examined was stuck with optical grease onto a phototube Philips XP 2020. The screen was then irradiated with fluorescent X-rays or γ-rays from radiactive sources (table II and III). Since the decay of luminescence in the $Gd_2O_2S(Tb)$ intensitying screens is about 500 μsec and this is a very long time when examined with the currently available electronic instruments for spectroscopy, we used the following instrumentation (see fig.3):

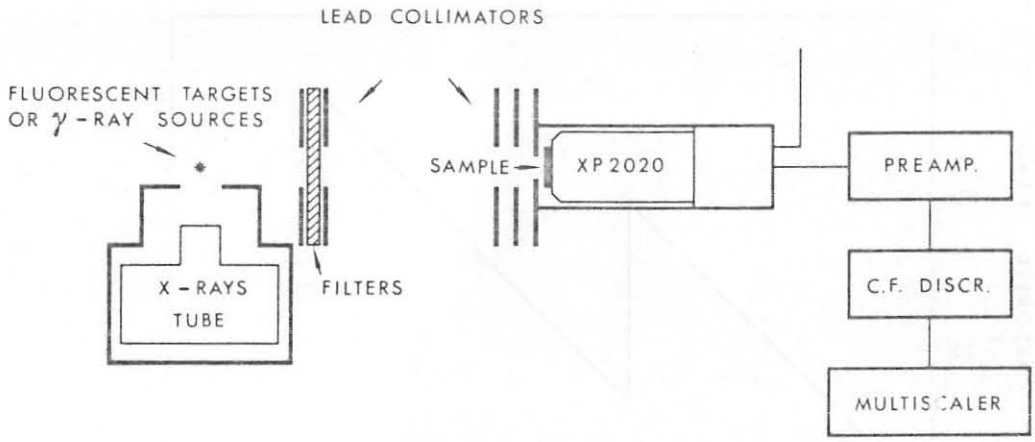

Fig. 3 - Schematic draw of the experimental arrangement.

signals from light pulses were delivered to a multichannel used as a multiscaler. The single electron pulses supplied by the anode of the phototube were timed and shaped by a constant fraction discriminator ORTEC with a threshold setting capable of discriminating the single electron signals from the noise.

After shaping, pulses were sent to the multiscaler adjusted to a channel time of 90 μsec and a stepping time of 100 μsec. In this way every individual light pulse covers a range of about 10 channels so that it is possible to show subsequent pulses on the 1017 channels of the multichannel (equivalent to 101,7 milliseconds) it is also possible to observe superimprosed pulses, the level of back-ground noise and the level of noise from the phototube.

Back-ground noise was considerably limited by a carefull lead shielding. To check the single electon response (SER) pulse count loss due to threshold setting in the disciminator, SER spectrum was measured in coincidence with single photon pulses emitted by a LED; the ratio between spectrum obtained at low threshold and at operational condition was also evaluated and resulted to be 1,2.

Fig. 4 shows a typical display of the multiscaler. The plot of light pulses obtained was then integrated, recorded and reported on a histogram with the number of electrons counted

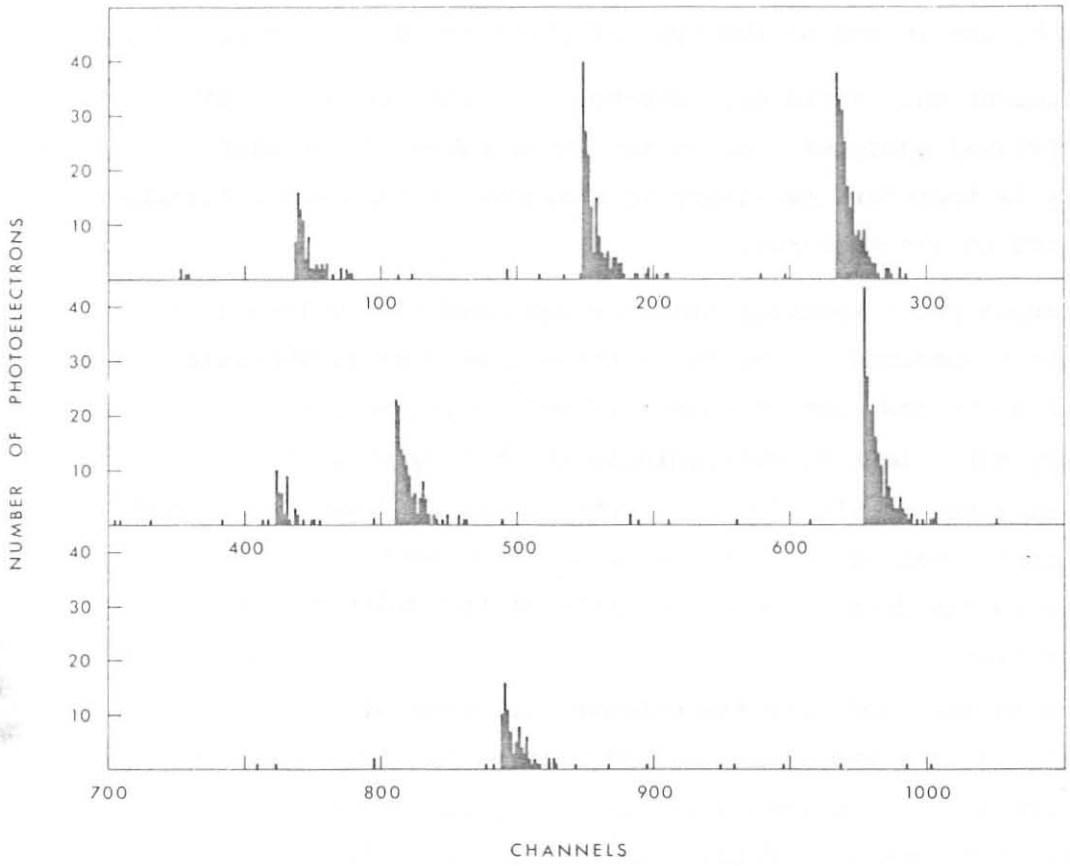

Fig. 4 - Typical data display on the multiscaler screen (the total sequence of 1017 channels is here divided in three parts reported from top to bottom.
On the X-axis every channel corrisponds to 100 μsec and is related to counts of single photoelectrons in the live-time of every channel (90 μsec) on the y-axis. See text.
Every peak corrisponds to an X-ray absorbed by the screen

every pulses versus the frequency of counts found; from this we obtained the typical spectrum of pulse height which is commonly seen in spectroscopy.

To find out the number of light photons emitted every individual flash, it is necessary to know the conversion efficiency of photons into photoelectrons.

This efficiency is a function of the wavelenght of the light emitted by the IS and of the type of photocathode in the phototube.

Moreover this efficiency depends upon the parameters of the individual phototube and varies among tubes of the same type; it is therefore necessary to evaluate it for each phototube being used in the measures.

A Broca prism spectrophotometer was used to develope this data with a specimen of the IS on the entrance slit. The screen was excited by radioactive source of Am^{241} with an output of intensity sufficient to discriminate the back-ground. At the output slit the previously used phototube XP 2020 was collimated. The equipment was set by the use of a sodium lamp so as to obtain also the definition as function of the width of the entrance slit.

Due to the fact that the emission spectrum of the Tb activated IS is a spectrum with very fine lines clustered in 6 main groups ([6]) the resolution of the system was varied to integrate the emission of the finest lines to achieve a maximum steady level of counts in corrispondence with every group of peaks.

The curves obtained by the above technique were corrected to account for the conversion efficiency related to the photo-cathode and normalized to the absolute value of efficiency at 401 nm (22,5%) as supplied by the manufacturer.

By a summation we obtain the total efficiency of the phototube used in detecting the light from the screens.

Low energy X-rays (10-30 keV) and those with energy immediately above the K-edge of Gd are strongly absorbed by the IS. By observing the distribution of points where interaction with X-rays takes place on a section of the screen cut in the direction of the X-ray beam, it can be noted that a higher mass absorption

coefficient corresponds to a higher distribution of interacting points toward the side of the source (Fig. 5).

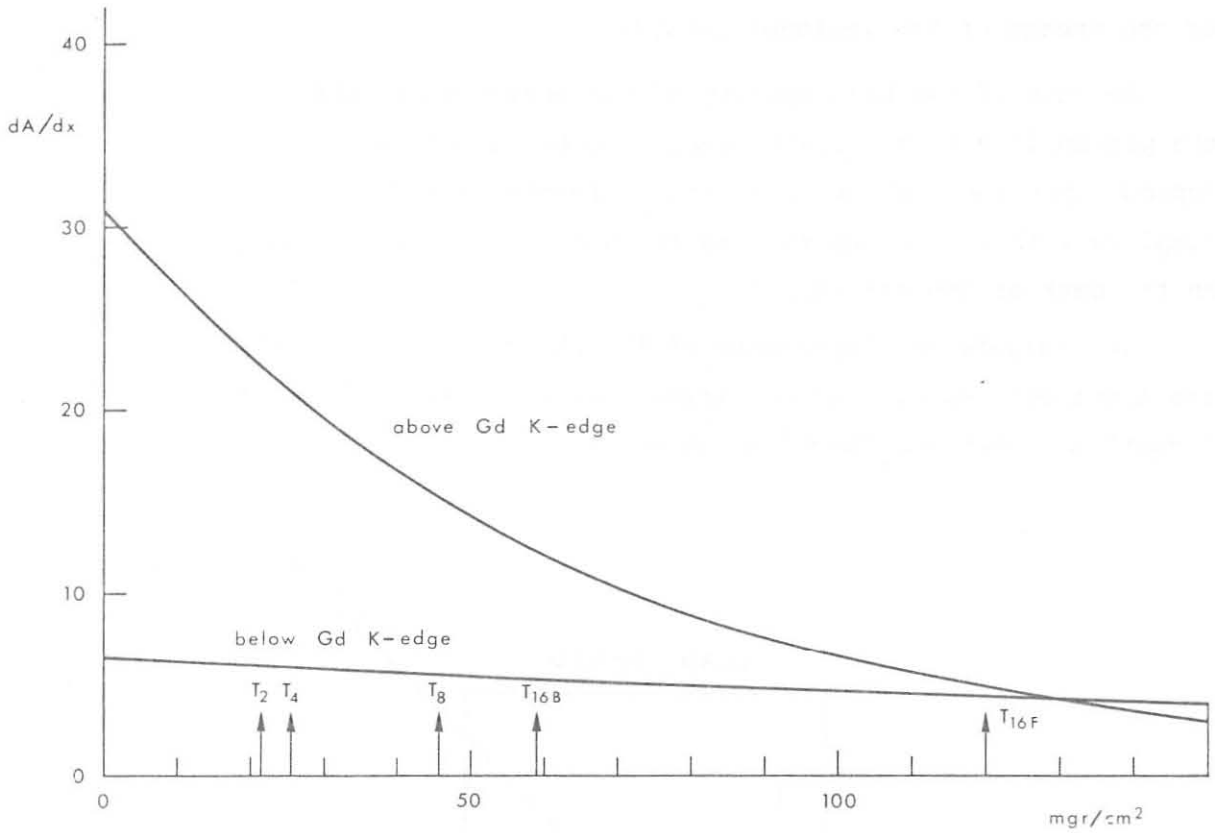

Fig. 5 - X-ray absorption in the cross-section of the screens. Two curves are reported relative to energy slightly above and below Gd K-edge. The X-axis gives the thickness of Gd_2O_2S (in ngr/cm^2) crossed by the X-rays. The different thickness of TRIMAX screens is also shown. The values of absorption per unit of thickness according to the formula

$$\frac{dA}{dX} = \frac{\mu}{\rho} \exp\left(-\frac{\mu}{\rho} x\right)$$

where A is the absorption and X the thickness, are given on the y-axis.

Because of this, the average free path of the photons to come out of the screen is larger if the source is opposite to the detector (film or phototube) and, in this setting, increases with the mass absorption coefficient being therefore a function of the energy of the incident X-rays.

Because of the high opacity of the phosphors of the screens the probability that a light photon comes out of the screen depends upon the average free path. A further element may complicate the issue and this is the use of a reflecting layer on the back of the screen.

To evaluate the importance of the phenomenon we measured the light emitted by a screen irradiated with X-rays from the "front" and from the "back" as shown in Fig. 6.

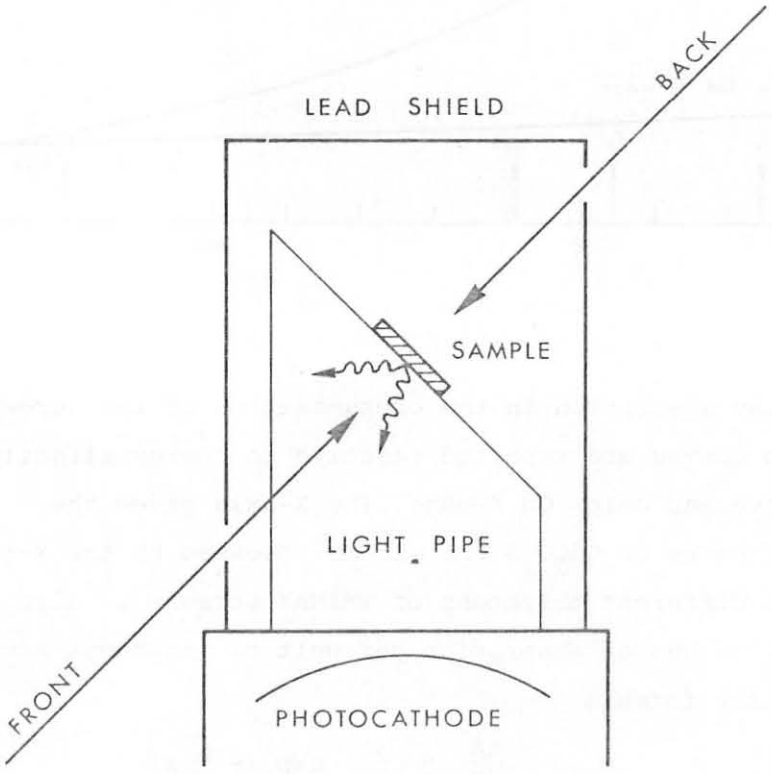

Fig. 6 - Experimental arrangement to evaluate the self--absorption of light inside the screen. Arrows represent the direction of X or γ radiation falling on the "back" and "front" on the screen.

The system developed allows us to exchange the source in the two positions shown as "back" and "front" without changing the light collecting device.

Since the light collecting efficiency is lower compared to previous arrangement (Fig. 3), the result have been adjusted to those obtained in that setting (back) and are shown in Fig.8 lowest graph.

Due to the limited amount of data available in the literature and to their disagreement on the thickness of screens ([2,7,8]) measures of transmission of screens were carried out by using a NaI spectrometer and three different radioactive sources in a very narrow emitting geometry and using a carefull shielding.

From the transmission data, the thickness (mg/cm^2) of the screens may be obtained by using the values of the mass absorption coefficient for Gd_2O_2S as obtained from ([4]) with the compound formula.

Values so obtained are compared with those in the literature in Table I. In Table III the reader may find sources and energy of X-rays that in this procedure have been used without filtering.

The most reliable data is felt to be that obtained by using the source of Am^{241} at 59,57 keV due to the almost inexistent noise level under the peak.

The counts on the full peak in other spectra have been measured with the method of the trapeze.

CHAPTER 3

DISCUSSION.

Some comments on the experimental data presented are necessary.

By considering the histogram in Fig. 7 (a+b) describing the spectrum of pulses obtained with the T_2 screen, it can be noted that, for energies below the K-edge, it is formed by a single peak whose average value (as number of photoelectrons every X-rays absorbed) increases almost linearly with the energy of the absorbed X-ray (see also Fig. 9). Also the resolution, defined as full width half maximum (FWHM), which is another relevant parameter in evaluating the spectroscopical quality of a detector, increases with energy, while ratio $\Delta E/E$, which should vary as a function of $1/\sqrt{E}$ is not too sensitive to changes in energy.

The overall process of conversion of the X-ray energy into emission of photoelectrons can not be described by a purely poissonian statistic, therefore we have to believe in the existence of some phenomenon in the process itself not following the statistic of Poisson.

The phenomena may be related to variations in the energy conversion of absorbed X-rays into ionization, these variations may be due to graininess of Gd_2O_2S, to non-homogeneous transformation of ionization into light by the luminescence centres of Tb, to the variations of light collection by the photocathode. The latter is dependent on the probability of a luminescent photon, emitted by a given point of the screen, to come out of the screen itself. The system photocathode-phototube does not show these kind of problems as it can be demostrated by the data obtained on the same phototube.

The same result may also be obtained by substituting the specimen of the screen with a NaI (Tl) crystal running a series of spectra with different sources.

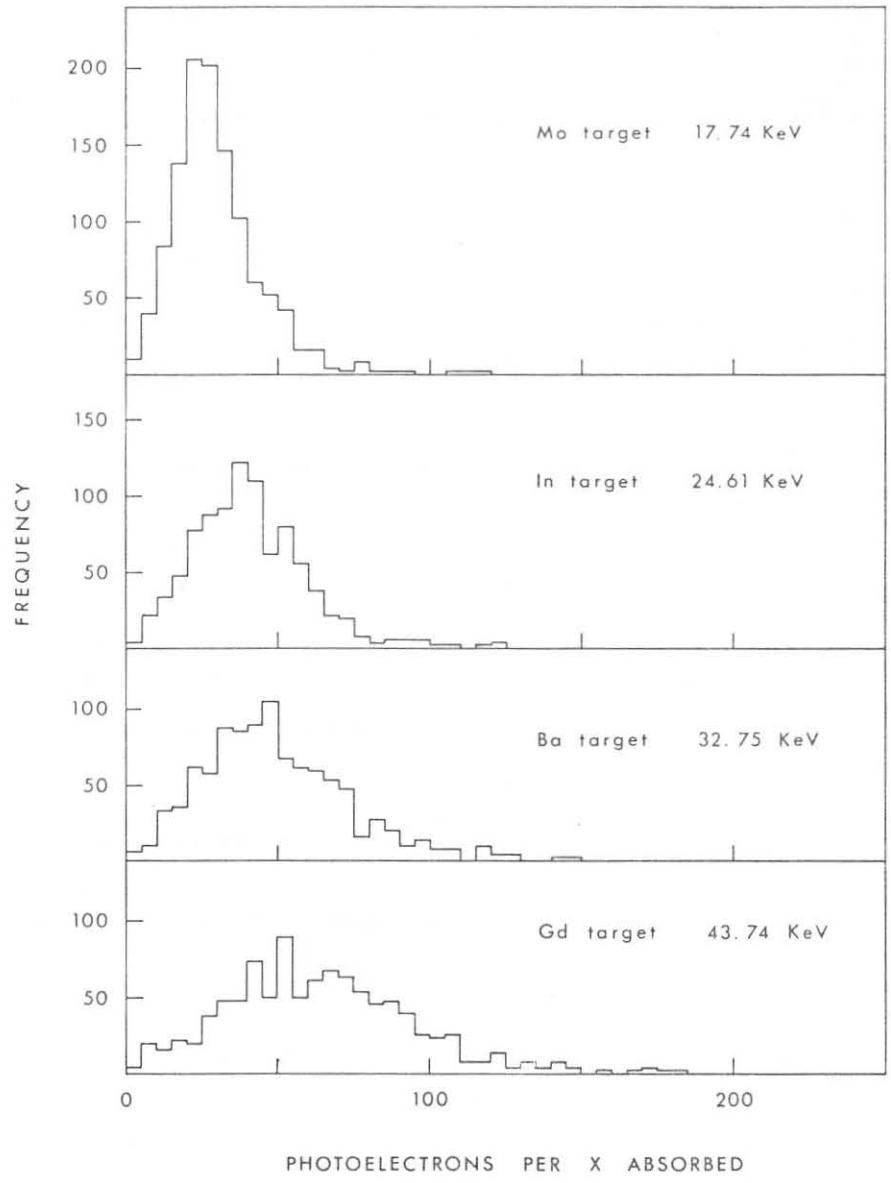

Fig. 7.a

Fig. 7(a+b) - Pulse height spectra for a T_2 Gd_2O_2S IS obtained with different X and γ rays from fluorescent targets and γ-sources, below (7a) and above (7b) Gd K-edge.

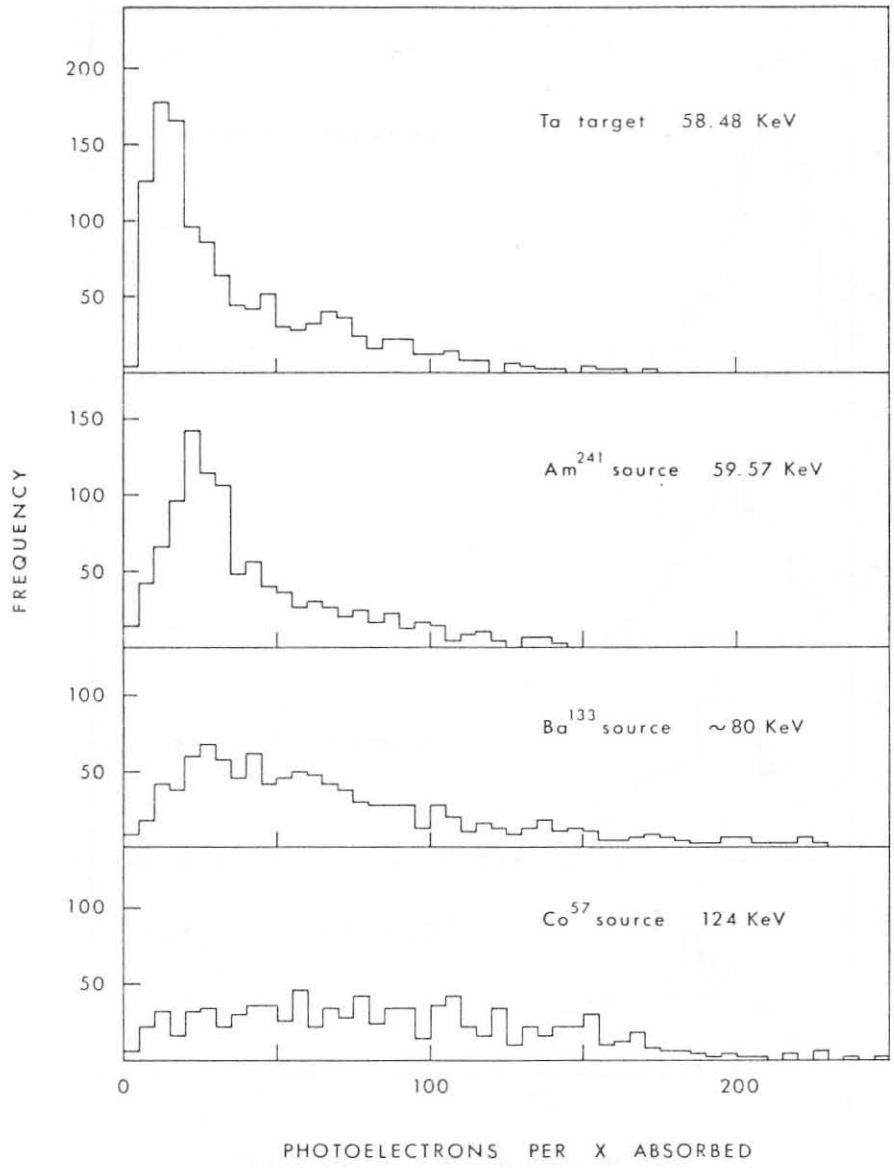

Fig. 7.b

Fig. 7(a+b) - Pulse height spectra for a T_2 Gd_2O_2S IS obtained with different X and γ rays from fluorescent targets and γ-sources, below (7a) and above (7b) Gd K-edge.

When examining the spectra obtained with the source of Am^{241}, about 60 keV (Fig. 8), for all the Trimax series, the distribution of the pulses appear to be divided into two components:

1. full energy peak component,
2. escape component.

The latter is due to the energy loss caused by the fluorescent X-ray escape out of the screen. For T_{16F} the two components appear to be very well separated because of the better conversion efficiency of the screen.

For T16B the shape of the pulse spectrum has an altered ratio between escape and full peak; this is probably due to the reabsorption of fluorescent X-ray as a consequence of the considerable thickness of this screen.

Moreover, by using a Co^{57} source, the poor spectroscopical performance of this screen plus the fluorescent X-ray loss and the escape of the high energy photoelectrons out of the screen, brings a rather flat spectrum which starts from the origin of the axis without escape or full peaks.

Data shown on Fig. 9 gives the different conversion efficiencies of X-ray energy into light photons. The highest efficiency is obtained with T_{16B} screen.

The peculiar feature of this diagram is the difference between efficiency values above and below K-edge; this difference is in accordance with theoretical data for the first four screens while there is less agreement in the case of T_{16B} screen.

This is confirmed in Fig. 9 where the results obtained with the T_{16B} screen put in the two positions indicated in Fig. 6 as "back" and "front", are reported on the same graph. Should the difference be due to phenomena of light absorption inside the screen, the result obtain when irradiating the screen from "front" would be higher versus those obtained when irradiating from the "back".

The phenomena of light absorption in the bulk of the

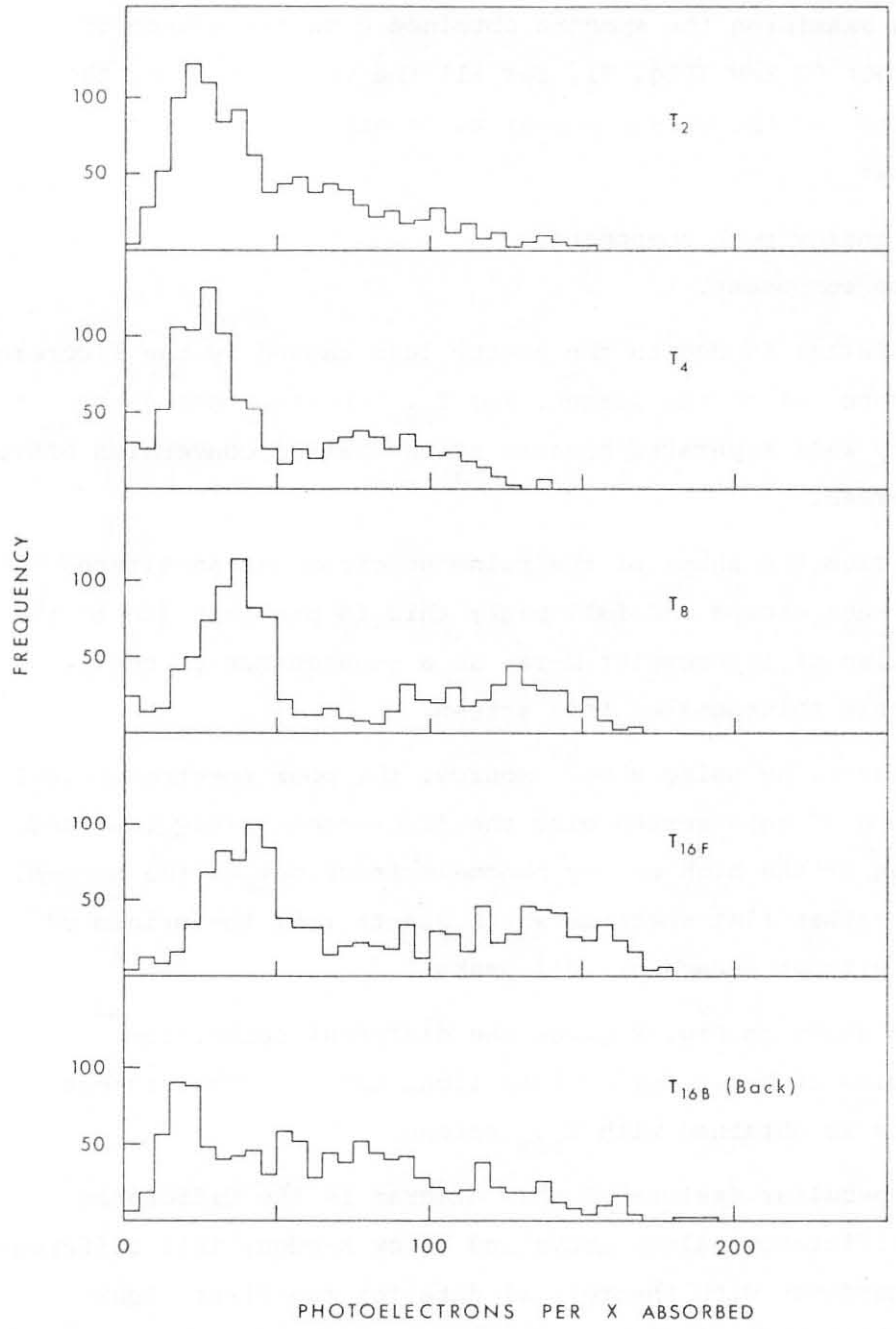

Fig. 8 - Pulse height spectra for the TRIMAX screens obtained with the use of Am^{241} (59,57 keV).

material constituting the screen are shown on Fig. 9 lower graph, where "front" values are always higher than "back" ones.

Similar measurements made for other screen do not give significant differences; this is due to their smaller thickness.

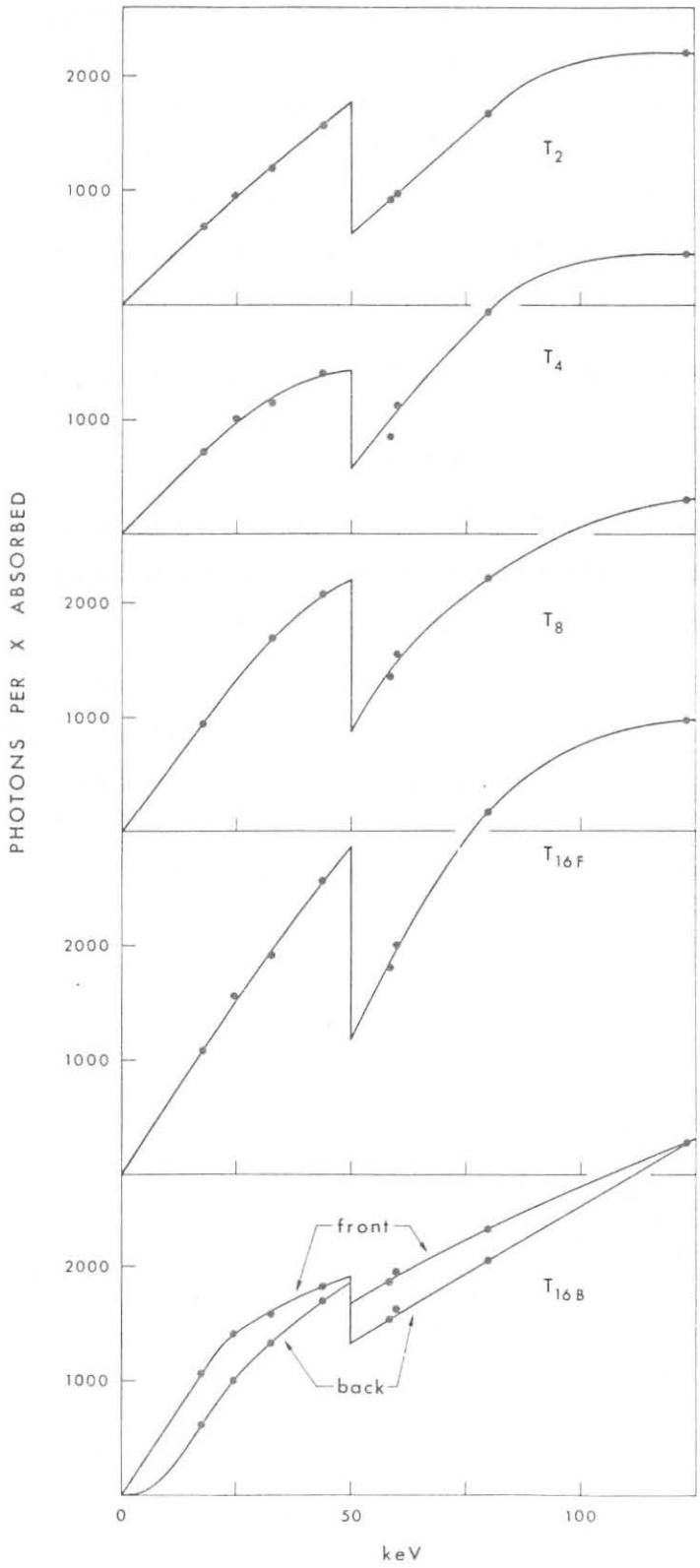

Fig. 9 - Light emission efficiency versus energy of absorbed X-rays for TRIMAX.

We have then obtained what we define "absolute speed curves" (ASC) as a function of the energy of incident X-rays, where the speed is meant to represent the number of photons emitted, every incident X-rays (Fig. 10). This was done by using the values of the mass absorption coefficient as obtained on the basis of data taken from ([4]) and from our values of screen thickness in mg/cm^2.

The mathematical expression of the "absolute speed curves" is:

$$S(E) = A(E) \times F(E)$$

where A(E) is the absorption efficiency, F(E) is the overall efficiency of light emission outside the screen each X-ray absorbed as a function of the energy of the X-ray itself.

In these curves we may note a peculiar behaviour of T_{16B} versus all other screens; this is due to its remarkably higher thickness and implies an absolute maximum for S(E) above K-edge. This value is the highest in both cases when irradiated from "front" or "back".

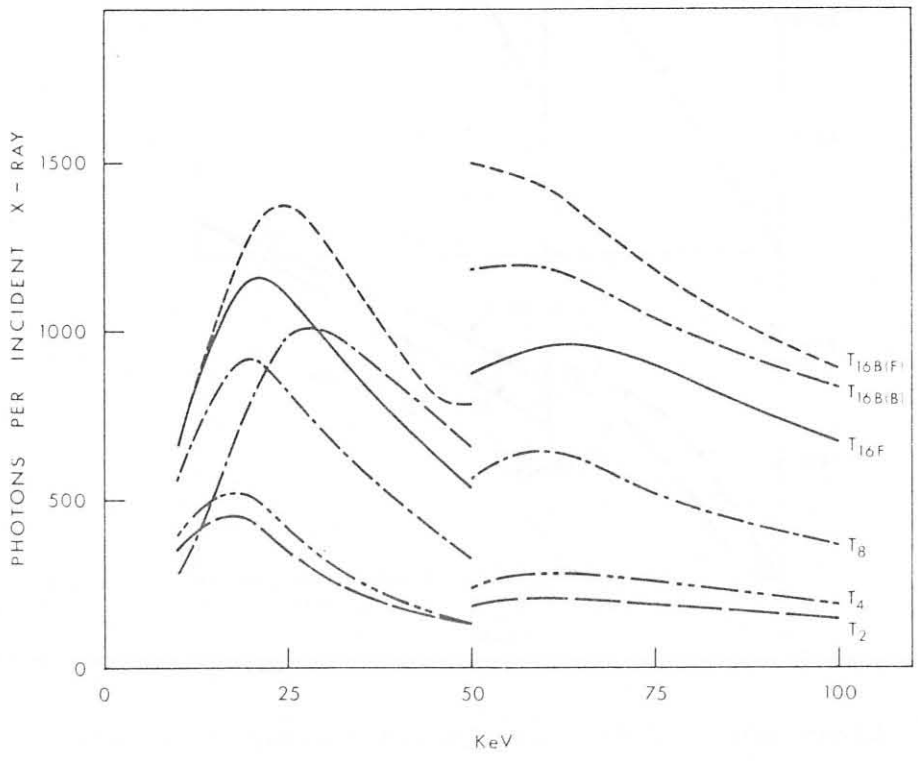

Fig. 10 - ASC for each TRIMAX IS. See text.

CHAPTER 4

CONCLUSIONS

The measures carried out on the physical characteristic of X-rays absorption, conversion into light, transmission of the light relative to TRIMAX allow us to draw "ASC" for every incident X-ray's energy.

These curves describe the overall efficiency of the different screens in the range of energies of interest.

The other feature stemmed from our investigation is the emission of fluorescent X-rays of high energy (45 keV) when the absorbed X-ray has energy higher than K-edge. This effect was overlooked in various early works on the rare-earth IS but it has a remarkable importance since it firstly causes a loss in the conversion efficiency above K-edge and in addition is responsible for a secondary radiation inside a MSTS. This radiation is numerically remarkable (about 80% of X-rays absorbed above the K-edge) and it can be reabsorbed at a significant distance from the place where is generated, this causing a poorer image quality.

TABLE I

THICKNESS OF TRIMAX IS (mg/sqcm)

T2	T4	T8	T16F	T16B	
21.5	25.5	45.7	59.0	120.0	this article
25.3	30.1	56.6	51.8	103.5	Birch et al. (1979)
		52.5			Venema (1979)

TABLE II

FLUORESCENT X-RAY TARGETS AND MEAN K X-RAY EFFECTIVE ENERGY

TARGET	K X-RAY ENERGY (keV)
Germanium	9.5
Molybdenum	17.74
Indium	24.61
Barium	32.75
Gadolinium	43.74
Tantalum	58.43

TABLE III

GAMMA RAY SOURCES , FILTERING & RELEVANT GAMMA RAY ENERGY

SOURCE	GAMMA RAY ENERGY(keV)	FILTERS
Am^{241}	59.57	Al
Ba^{133}	80.00	Al + In
Co^{57}	124.00	Al

BIBLIOGRAPHY

(1) Oggioni R. 1979 La Radiologia Medica Suppl. 2 189-193.

(2) Birch R. Marshall M and Ardran GM 1979 Catalogue of spectral data for diagnostic X-rays (The Hospital Physicists' Association SRS-30) 132-139.

(3) Evans RD. 1968 in Radiation Dosimetry vol. I, ed. FH Attrix, WC Roesch and Tochilin E. (New York and London: Academic Press) pp. 93-155.

(4) Storm E. and Israel HI 1970 Nuclear Data Tables A7, 565-681

(5) Morlotti R. 1975 J. Phot. Sci. 23, 181-189.

(6) Stevels ALN. 1975 Medicamundi 20 12-22

(7) Venema HW. 1979 Radiology 130 765-771

(8) Giacomich R., Tomasini F., Bacarini L., Di Lelio A. 1982 Radiol. Med. 68 571-580.